Fidelity of the quantum δ-kicked accelerator

R. K. Shrestha, S. Wimberger, J. Ni, W. K. Lam, and G. S. Summy

Fidelity of the quantum delta-kicked accelerator

R. K. Shrestha,[1] S. Wimberger,[2] J. Ni,[1] W. K. Lam,[1] and G. S. Summy[1]

[1]*Department of Physics, Oklahoma State University, Stillwater, Oklahoma 74078-3072, USA*
[2]*Institut für Theoretische Physik, Universität Heidelberg, Philosophenweg 19, 69120 Heidelberg, Germany*

The sensitivity of the fidelity in the kicked rotor to an acceleration is experimentally and theoretically investigated. We used a Bose-Einstein condensate exposed to a sequence of pulses from a standing light wave followed by a single reversal pulse in which the standing wave was shifted by half a wavelength. The features of the fidelity "spectrum" as a function of acceleration are presented. This work may find applications in the measurement of temperature of an ultra-cold atomic sample.

The study of non-linear systems is important to many branches of science. Consequently the chaotic behavior that they can exhibit in the classical regime has been extensively studied and used [1–3]. A particularly interesting aspect of such systems is that due to the linearity of the Schrödinger equation, their quantum and classical dynamics can be dramatically different. For this reason the so called delta-kicked rotor and its quantum analog the quantum delta-kicked rotor (QDKR) have received much attention. The latter can be experimentally realized by subjecting a sample of cold atoms to short pulses of an off-resonant standing wave of laser light [4]. The QDKR has proved to be a paradigmatic model to study several important phenomena including quantum resonances (QR) [5, 6], dynamical localization [5, 7], and quantum ratchets [8]. A closely related system, the quantum delta kicked accelerator (QDKA), differs from the usual QDKR by adding a linear potential in the form of an acceleration. The QDKA has been used in studying aspects of the transition to chaos in both classical and quantum regimes [9], and is a system in which quantum accelerator modes [10, 11] are observed.

One of the common themes in the experiments mentioned above is that the quantum evolution is typically measured indirectly through observations of the momentum distribution. However recently it has become possible to study the coherent evolution of a superposition of state vectors directly by examining the overlap of the atomic state with a reference state. This quantity is termed "fidelity". It has garnered considerable interest as an alternative way of studying coherent evolution in the context of quantum-classical correspondence [12] and quantum information processing [13]. Recently, it was shown that the width of a pulse-period fidelity resonance of the QDKR exhibits sub-Fourier scaling [14, 15], where the width of the resonance scales as the inverse cube of the number of applied pulses. Because of this sensitivity to the pulse period, the fidelity technique was proposed as a means for improving the precision of frequency measurements [15]. Although subsequent work has shown possible limitations with this approach [16], we show here that the observed asymmetry in the fidelity with respect to an acceleration may be used for temperature measurements of the atomic cloud.
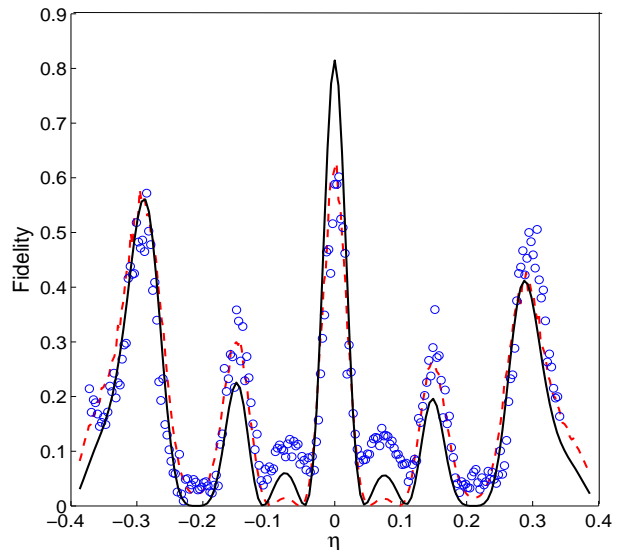

FIG. 1. (Color Online) Fidelity as a function of the scaled acceleration, η, due to four kicks of strength $\phi_d \approx 0.6$ followed by a reversal kick of strength $\approx 4\phi_d$. The black solid (red dashed) line is a numerical simulation with $\tau = 2\pi$ (i.e. $\ell = 1$), $\beta = 0.5$ and initial momentum width $\Delta\beta = 0.06\hbar G$ without (with) effects such as vibrations and reversal phase imperfections (see more in the text). Circles are experimental data. Note that the fidelity has a rich structure with multiple resonant peaks. All fidelity measurements are ± 0.01.

In this paper we discuss the sensitivity of fidelity in the QDKA to an externally applied acceleration. A full analytical theory (neglecting atomic interactions) along with corresponding experimental results and numerical simulations are presented. We show that the width of resonant peaks in fidelity as a function of acceleration are sensitive to the momentum width of the atomic sample, the pulse period, and the direction of the acceleration.

The dynamics of the kicked accelerator can be described by a Hamiltonian which in dimensionless units
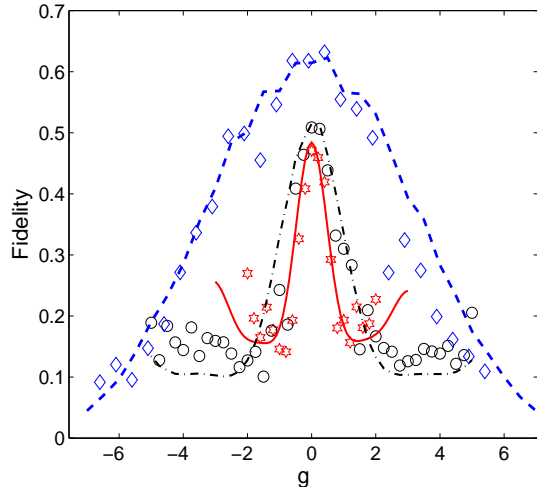
FIG. 2. (Color Online) Plot showing the fidelity as a function of acceleration. Experimentally measured fidelity for $\ell = 1$ (blue diamonds), $\ell = 2$ (black circles) and $\ell = 3$ (red stars) due to four kicks of strength $\phi_d \approx 0.6$ followed by a reversal kick of strength $\approx 4\phi_d$. The lines are the corresponding fidelity from numerical simulations with $\Delta\beta = 0.06\hbar G$. Note that the horizontal axis is the real acceleration in order to show the reduction in the peak width as ℓ increases.

is [10]:

$$\hat{H} = \frac{\hat{p}^2}{2} - \frac{\eta}{\tau}\hat{x} + \phi_d \cos(\hat{x}) \sum_{q=1}^{\mathrm{t}} \delta(t' - q\tau). \quad (1)$$

Here $\hat{p}$ is the momentum in units of $\hbar G$ (two photon recoils) that an atom of mass M acquires from t short, periodic pulses of a standing light wave with a grating vector $G = (4\pi/\lambda)\sin\theta$ (θ is the angle made by each beam with the vertical). Other variables are the position $\hat{x}$ (in units of G^{-1}), and the continuous time variable t' (integer units). The pulse period T is scaled by $T_{1/2} = 2\pi M/\hbar G^2$ (the half-Talbot time) to give the scaled pulse period $\tau = 2\pi T/T_{1/2}$. Here we only consider pulse periods which are integer multiples of $T_{1/2}$, i.e. $\tau = 2\pi l$, l is integer. The strength of the kicks is given by $\phi_d = \Omega^2 \Delta t/8\delta_L$, where Δt is the pulse length, Ω is the Rabi frequency, and δ_L is the detuning of the kicking light from the atomic transition. Finally the scaled acceleration is defined as $\eta = \frac{MgT}{\hbar G}$, with g being the acceleration of the atoms relative to the standing wave.

In the absence of acceleration, the above Hamiltonian reduces to the standard kicked rotor system. Due to the spatial periodicity of the kicking potential the momentum can be decomposed as $p = n + \beta$ where n is the integer part of the momentum and β ($0 \leq \beta < 1$) is the quasi-momentum. The spatial periodicity of the kicking potential only allows the transition between momenta that differ by an integer multiple of two photon recoils, $\hbar G$, ensuring the conservation of quasi-momentum. The

dynamics of any single value of the quasi-momentum is the same as that of a rotor known as a $\beta-$rotor.

With a non-zero acceleration, the kicked particle becomes the kicked accelerator and the quantum dynamics of the system can be understood by applying the one-step operator, $\hat{\mathcal{U}}_{\beta,\phi_d,\eta}(\mathrm{t}) = e^{-i\phi_d \cos\hat{\theta}} e^{-i\frac{\tau}{2}(\hat{\mathcal{N}} + \beta + \eta\mathrm{t} + \eta/2)^2}$, where $\hat{\theta} = \hat{x} \mod (2\pi)$ and $\hat{\mathcal{N}} = -i\frac{d}{d\theta}$ is the angular momentum operator quantized by integers n. $\hat{\mathcal{U}}_{\beta,\phi_d,\eta}(\mathrm{t})$ is time dependent implying that the quasi-momentum will no longer be conserved. However, its conservation can be restored by writing Eq. (1) in a freely falling frame using a gauge transformation. The Hamiltonian then becomes,

$$\hat{\mathcal{H}}(\hat{\mathcal{N}}, \hat{\theta}, t') = \frac{1}{2}\left(\hat{\mathcal{N}} + \beta + \eta\frac{t'}{\tau}\right)^2 + \phi_d \cos(\hat{\theta})\sum_{q=1}^{\mathrm{t}}\delta(t'-q\tau). \quad (2)$$

In the current fidelity experiments, the initial state $|\psi(0)\rangle$ is kicked t times, each kick having a strength ϕ_d. At the end of the tth kick a single pulse with strength $t\phi_d$ is applied. We will refer to this as the "reversal kick" and it can be implemented by shifting the standing wave by $\lambda_G/2$. Thus the fidelity for a particular $\beta-$rotor is: $F(\eta, \mathrm{t}) = |\langle\psi(0)|\hat{\mathcal{U}}_{\beta,\mathrm{t}\phi_d,\eta=0}^{\dagger}\hat{\mathcal{U}}_{\beta,\phi_d,\eta}^{\mathrm{t}}|\psi(0)\rangle|^2$. Following the technique introduced in [17], the final expression for the fidelity is then given by,

$$F(\eta, \mathrm{t}) = \left| e^{-i\phi(\beta,\eta,\mathrm{t}) - in_0\ell\pi(2\beta+1)(\mathrm{t}-1) - i\ell\pi n_0\eta\mathrm{t}^2} \right.$$
$$\left. J_0\left(\sqrt{(\mathrm{t}\phi_d)^2 + \phi_d^2|W_\mathrm{t}|^2 - 2\mathrm{t}\phi_d^2\mathrm{Re}W_\mathrm{t}}\right)\right|^2, \quad (3)$$

where $p_0 = n_0 + \beta$ is the initial momentum of the plane wave, $\phi(\beta,\eta,\mathrm{t}) = \ell\pi\sum_{q=0}^{\mathrm{t}-1}(\beta + q\eta + \eta/2)^2$ is the global phase and $W_\mathrm{t}(\beta,\eta) = \sum_{q=0}^{\mathrm{t}-1}e^{-i[(2\beta+1)\ell\pi]q - 2\ell\pi iq\eta\mathrm{t} + i\ell\pi\eta q^2}$. In the limit $\eta \to 0$ for $\ell = 2$ and $\beta = 0$, the general result in Eq. (3) reduces to the special case considered in [15]. Equation (3) allows for consideration of situations in which the initial state is a mixture of plane waves. Here this state is assumed to have a Gaussian quasi-momentum distribution with a FWHM $= \Delta\beta$. For a given distribution $\rho(\beta)$ of the quasi-momentum, the formula for fidelity is generalized as: $F(\eta, \mathrm{t}) = \left|\int_0^1 \rho(\beta)\langle\psi(0)|\hat{\mathcal{U}}_{\beta,\mathrm{t}\phi_d,\eta=0}^{\dagger}\hat{\mathcal{U}}_{\beta,\phi_d,\eta}^{\mathrm{t}}|\psi(0)\rangle d\beta\right|^2$, where the average is computed numerically based on Eq. (3) [17, 18]. From the global phase term, $\phi(\beta,\eta,\mathrm{t})$, it can be seen that when $\beta \neq 0$ the phase induced by different values of η depends not only on the magnitude of η but also on its sign.

Our experiments to investigate this system were performed using a similar set up to that described in [15, 19]. A Bose-Einstein condensate (BEC) of about 40000 ^{87}Rb atoms was created in the $5S_{1/2}$, $F = 1$ level using an all-optical trap technique. Approximately 5 ms after being released from the trap, the condensate was exposed to a pulsed horizontal standing wave. This was formed by two laser beams of wavelength $\lambda = 780$ nm, detuned 6.8GHz
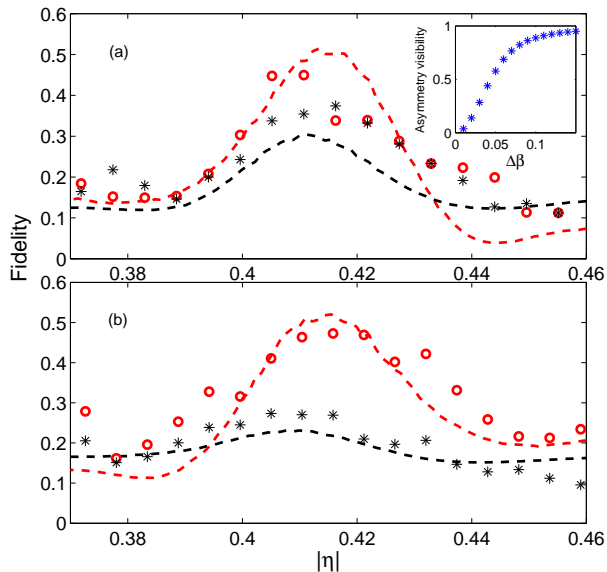
FIG. 3. (Color Online) Fidelity as a function of η for $\tau = 4\pi$ and $\beta = 0.5$. Red circles and black stars represent experimental fidelity with negative and positive accelerations respectively. Panels (a) and (b) correspond to different $\Delta\beta$ (panel (b) with higher $\Delta\beta$). The measurements were done with four kicks of strength $\phi_d \approx 0.6$ followed by a reversal kick of strength $\approx 4\phi_d$. The dashed lines are the simulations for (a) $\Delta\beta = 0.06\hbar G$, and (b) $\Delta\beta = 0.07\hbar G$. The inset shows the asymmetry visibility (see text) as a function of $\Delta\beta$.
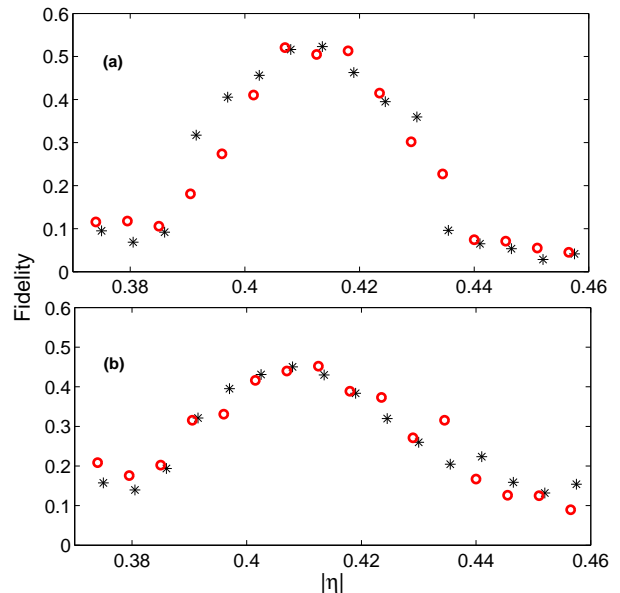

FIG. 4. (Color Online) Same as in Fig. 3 but for the center of the quasi-momentum distribution at $\beta = 0$. Note that in contrast to Fig. 3 there is no asymmetry between the positive and negative η's.

to the red of the atomic transition. The direction of each beam was aligned at 53º to the vertical. With these parameters the primary QR (half-Talbot time [20, 21], $\tau = 2\pi$) occurred at multiples of 51.5±0.05 µs. Each laser beam passed through an acousto-optic modulator driven by an arbitrary waveform generator. This enabled control of the phase, intensity, and pulse length as well as the relative frequency between the kicking beams. Adding two counterpropagating waves differing in frequency by Δf resulted in a standing wave that moved with a velocity $v = 2\pi\Delta f/G$. Since the quasi-momentum β of the BEC relative to the standing wave is proportional to v, changing Δf enabled β to be systematically controlled.

The kicking pulse sequence is similar to that described in [15]. The atoms were exposed to a set of t periodic pulses (forward pulses) each of length 1.08 µs and kicking strength ϕ_d followed by the reversal pulse (standing wave displaced by $\lambda_G/2$) with a strength tϕ_d. We varied the intensity rather than the pulse length to change the kicking strength ϕ_d. This was done by adjusting the amplitudes of the RF waveforms driving the kicking pulses. This ensured that the experiments were always performed in the Raman-Nath regime (the distance an atom travels during the pulse is much smaller than the spatial period of the potential). Finally the kicked atoms were absorption imaged in a time-of-flight experiment and the fraction of

atoms which returned to the initial momentum state was determined. Experimentally the fidelity was defined as $F = p_0/\sum_n p_n$ where p_n is the number of atoms in the nth momentum order. The value of $\Delta\beta$ was varied by changing the power of the CO_2 laser beam which formed the dipole trap used to realize evaporative cooling in the experiment. By adjusting the power of the laser for the final step in the evaporative sequence we were able to change $\Delta\beta$.

Figure 1 shows the experimentally measured fidelity as a function of acceleration for $\ell = 1$ and initial momentum $\beta = 0.5$ due to four kicks each of strength $\phi_d \approx 0.6$ followed by a reversal kick of strength $\phi_d \approx 2.4$. Numerical simulations were performed with these experimental parameters under two different conditions. First the black solid line is a simulation in which the reversal pulse is perfect in amplitude (amplitude = tϕ_d), and there are no random phase variations in the standing wave that could be caused by vibrations of the optics used to form it. In order to attempt to explain the large deviation of this simulation from the experiment, we also carried out a simulation in which the above experimental imperfections were included (red dashed line). Here we used experimentally realistic values of strength of the reversal kick (±7% from the ideal kick strength) and a random phase variation due to vibrations of 0.02π per pulse. As can be seen the fit to the experiment is quite good, leading us to believe that these effects are the most likely reason for the black curves poor match to the experiment at the $\eta = 0$ resonance. In the simulations that follow, we will employ the method used to generate the

red dashed curve (with the same parameters for the experimental imperfections).

Unlike in previous work where only the central resonance was observed [14, 15], it is now possible to see that the fidelity has a more complex structure with many resonances away from $\eta = 0$. The validity of the theory for higher resonances at $\ell = 2$ and 3 was also tested, the results of which are presented in Fig. 2. Due to the longer time available for momentum state phases to evolve at the larger ℓ, the peaks become narrower as ℓ is increased. Note that the fidelity is presented as as a function of real acceleration in order to show this effect.

We also examined the dependence of the fidelity to the sign of η (positive and negative acceleration). Asymmetry as predicted by the above theory after Eq. (3) was observed when the $\beta-$rotor distribution was centered at $\beta = 0.5$. It became more prominent as $\Delta\beta$ was increased as shown in Fig. 3. Note that the results correspond to pulse periods, $\tau = 4\pi$ ($\ell = 2$). The origin of the asymmetry is the different phases $\phi(\beta, \eta, \mathrm{t})$ induced by the negative and positive values of acceleration. Figure 3 shows the development of the asymmetry, both in the experiment and simulations, as $\Delta\beta$ is increased. The dashed lines are the plot of the simulations with $\Delta\beta = 0.06\hbar G$ and $0.07\hbar G$ (panels (a) and (b) respectively). An "asymmetry visibility" defined as $(F(\eta_-) - F(\eta_+))/(F(\eta_-) + F(\eta_+))$ shows an almost linear scaling with the momentum width ($\Delta\beta \leq 0.08\hbar G$) of the cloud (see inset). Thus measurement of the asymmetry may provide a means of determining small $\Delta\beta$ and hence the temperature of ultra-cold atomic clouds. Interestingly, the asymmetry goes away if the initial β distribution is chosen centered at $\beta = 0$ as is possible for $\ell = 2$ (see Fig. 4) for the same two $\Delta\beta$'s used in Fig. 3. In this case, the distribution is symmetric so that the distribution on the negative side is identical to that on the positive side. Thus changing the sign of the acceleration, η, has no effect on the dynamics. However with the β distribution centered at any value other than zero, the distribution is no longer symmetric and the effect of η will be different for each half of the β distribution.

In conclusion, we performed an experimental investigation on the sensitivity of the fidelity to the acceleration by exposing a BEC to a set of delta-kicked rotor optical pulses followed by a stronger reversal pulse. The experimental results and analytical theory were in good agreement with both showing the presence of multiple fidelity resonances. The width of the central fidelity resonance was found to become narrower as the pulse period increased. The importance of the position of the center of the initial momentum distribution was also explored. When the distribution was centered at some values other than zero, an asymmetry between the fidelity at positive and negative values of acceleration was observed which became more prominent with increasing $\Delta\beta$. The asymmetry was optimum for a distribution centered at $\beta = 0.5$, disappearing almost completely when the distribution was centered at $\beta = 0$. These findings can be used to determine the temperature of ultra-cold atoms, based on the scaling of the asymmetry with $\Delta\beta$ (inset in Fig. 3).

[1] M. C. Gutzwiller, *Chaos in Classical and Quantum Mechanics*, (Springer-Verlag, New york, 1990).

[2] B. V. Chirikov, Phys. Rep. **52**, 263, (1979).

[3] G. Casati *et al.*, *Stochastic Behavior of a Quantum Pendulum Under a Periodic Perturbation*, in Stochastic Behavior in Classical and Quantum Hamiltonian Systems, edited by G. Casati and J. Ford (Springer, Berlin, 1979), p. 334.

[4] F. L. Moore *et al.*, Phys. Rev. Lett. **75**, 4598 (1995).

[5] F. L. Moore *et al.*, Phys. Rev. Lett. **73**, 2974 (1994).

[6] C. Ryu *et al.*, Phys. Rev. Lett. **96**, 160403 (2006); F. M. Izrailev, Phys. Rep. **196**, 299 (1990); W. H. Oskay *et al.*, Opt. Comm. **179**, 137 (2000).

[7] J. Ringot *et al.*, Phys. Rev. Lett. **85**, 2741 (2000).

[8] I. Dana *et al.*, Phys. Rev. Lett. **100**, 024103 (2008); R. D. Astumian and P. Hänggi, Phys. Today **55**, No.11, 33 (2002); M. Sadgrove *et al.*, Phys. Rev. Lett. **99**, 043002 (2007); I. Dana and V. Roitberg, Phys. Rev. E. **76**, 015201(R) (2007); E. Lundh and M. Wallin, Phys. Rev. Lett. **94**, 110603 (2005).

[9] L. E. Reichl, *The Transition to Chaos*, 2nd ed.(Springer, Newyork, 2004).

[10] S. Fishman, I. Guarneri and L. Rebuzzini, Phys. Rev. Lett. **89**, 084101 (2002); J. Stat. Phys. **110**, 911 (2003).

[11] G. Behinaein *et al.*, Phys. Rev. Lett. **97**, 244101 (2006); V. Ramareddy *et al.*, Euro. Phys. Lett. **89**, 33001 (2010); M. K. Oberthaler *et al.*, Phys. Rev. Lett. **83**, 4447 (1999); P. Ahmadi *et al.*, Phys. Rev. A **80**, 053418 (2009).

[12] R. A. Jalabert and H. M. Pastawski, Phys. Rev. Lett. **86**, 2490 (2001); N. R. Cerruti and S. Tomsovic, Phys. Rev. Lett. **88**, 054103 (2002).

[13] M. A. Nielsen and I. L. Chuang, *Quantum Computation and Quantum Information* (Cambridge University Press, Cambridge, 2001).

[14] P McDowall *et al.*, New J. Physics. **11**, 123021 (2009).

[15] I. Talukdar, R. Shrestha, and G. S. Summy, Phys. Rev. Lett. **105**, 054103 (2010).

[16] R. A. Horne, R. H. Leonard, and C. A. Sackett, Phys. Rev. A **83**, 063613 (2011).

[17] S. Wimberger and A. Buchleitner, J. Phys. B **39**, L145 (2006); R. Dubertrand, I. Guarneri, and S. Wimberger, Phys. Rev. E **85**, 036205 (2012).

[18] S. Wimberger *et al.*, Nonlinearity **16**, 1381 (2003).

[19] R. K. Shrestha, J. Ni, W. K. Lam, S. Wimberger, and G.

S. Summy, Phys. Rev. A **86**, 043617 (2012).

[20] M. Lepers, V. Zehnlé, and J. C. Garreau, Phys. Rev. A

77, 043628 (2008).

[21] L. Deng *et al.*, Phys. Rev. Lett. **83**, 5407 (1999).